

Synthesis of  $\pi$ -Conjugated Polymers Containing Organoboron Benzo[*h*]quinolate in the Main Chain

Yuichiro Tokoro, Atsushi Nagai, and Yoshiki Chujo\*

Department of Polymer Chemistry, Graduate School of Engineering, Kyoto University, Katsura, Nishikyo-ku, Kyoto 615-8510, Japan

Received April 14, 2010; Revised Manuscript Received June 19, 2010

## Introduction

Organoboron dyes have recently found widespread interest as species with promising optical properties in various fields. They have been used as chemical probes,<sup>1</sup> photosensitizers,<sup>2</sup> and optical sensing<sup>3</sup> due to high luminescent quantum yields, large extinction coefficients, or two-photon absorption cross section. Among them, organoboron quinolates such as 8-hydroxyquinolinatediphenylboron (BPh<sub>2</sub>q)<sup>4</sup> turned out to be attractive as an alternative to tris(8-hydroxyquinolate)aluminum (Alq<sub>3</sub>)<sup>5</sup> for organic light-emitting diodes (OLEDs) because of their good thermal stabilities as well as the high emission quantum yields. BPh<sub>2</sub>q and their derivatives emit intense light from a quinoline-based intraligand charge transfer (ILCT) excited state.<sup>6</sup> This ILCT state is formed when the highest occupied molecular orbital (HOMO) and the lowest unoccupied molecular orbital (LUMO) are localized on the phenolate ring and on the pyridyl ring of the quinoline ligand, respectively. Introduction into polymers by covalent bonding is expected to be advantageous because of the improved processability such as film formability, thermal stability, and photostability, etc. Jäkke et al. first reported the synthesis of well-defined polymers incorporated into the polystyrene side chain via multistage polymeric reaction of poly(4-dibromoborylstyrene),<sup>7</sup> and Weck et al. also proposed the potentiality of organoboron quinolate-functionalized polystyrene as the excellent precursors for OLEDs.<sup>8</sup>

Recently, we have also prepared organoboron quinolate-containing conjugated polymers, in which *p*-phenyleneethynylene units were embedded to boron atoms in the polymer backbones.<sup>9</sup> Those polymers gave strong green fluorescence, and an efficient energy migration from conjugated linkers with high molar absorption coefficient to boron quinolate moieties was observed. Substituting groups on the Q-ligand moiety can change the emission color of the polymers; i.e., polymers with methyl-substituted organoboron quinolate polymers exhibited green-blue or blue photoluminescence.<sup>10</sup> Elements such as oxygen, sulfur, and selenium also affect the emission wavelength of the organoboron quinolate polymer.<sup>11</sup> Increasing of atomic number of the 16 group atom adjacent to the boron atom caused emission shift to longer wavelength and decreasing of absolute quantum yields for both the low-molecular-mass model compounds and the polymers.

Extension of  $\pi$ -conjugation is another important approach to changing the emission color. 10-Hydroxybenzo[*h*]quinoline can be regarded as a  $\pi$ -extended 8-hydroxyquinoline and shows proton transfer emission resembling to the emission from ILCT state,<sup>12</sup> so that 10-hydroxybenzo[*h*]quinolinatediphenylboron and the benzo[*h*]quinoline-containing polymers seem to be a

reasonable candidate for that aim, i.e., color change via the extended  $\pi$ -conjugated system of Q-ligand. Herein, we wish to report novel synthesis of 10-hydroxybenzo[*h*]quinolinatediphenylboron (**1**) and the incorporation of **1** into  $\pi$ -conjugated polymer backbone and discuss their optical properties in comparison with BPh<sub>2</sub>q.

## Experimental Section

**Measurements.** <sup>1</sup>H (400 MHz), <sup>13</sup>C (100 MHz), and <sup>11</sup>B (128 MHz) NMR spectra were recorded on a JEOL JNM-EX400 spectrometer. <sup>1</sup>H and <sup>13</sup>C NMR spectra used tetramethylsilane (TMS) as an internal standard; <sup>11</sup>B NMR spectra were referenced externally to BF<sub>3</sub>OEt<sub>2</sub> (sealed capillary) in CDCl<sub>3</sub>. The number-average molecular weight (*M<sub>n</sub>*) and the molecular weight distribution [weight-average molecular weight/number-average molecular weight (*M<sub>w</sub>/M<sub>n</sub>*)] values of all polymers were estimated by size-exclusion chromatography (SEC) with a TOSOH G3000HXL system equipped with three consecutive polystyrene gel columns [TOSOH gels:  $\alpha$ -4000,  $\alpha$ -3000, and  $\alpha$ -2500] and ultraviolet detector at 40 °C. The system was operated at a flow rate of 1.0 mL/min, with tetrahydrofuran as an eluent. Polystyrene standards were employed for calibration. UV–vis spectra were recorded on a Shimadzu UV-3600 spectrophotometer. Fluorescence emission spectra were recorded on a HORIBA JOBIN YVON Fluoromax-4 spectrofluorometer, and the absolute quantum yield was calculated by the integrating sphere method on the HORIBA JOBIN YVON Fluoromax-4 spectrofluorometer in chloroform. FT-IR spectra were obtained using a SHIMADZU IRPrestige-21 infrared spectrometer. Thermogravimetric analyses (TGA) were performed on a Seiko TG/DTA 6200 at a scan rate of 10 °C/min. X-ray crystallographic analysis was carried out by a Rigaku R-AXIS RAPID-F graphite-monochromated Mo K $\alpha$  radiation diffractometer with an imaging plate. A symmetry related absorption correction was carried out by using the program ABCOR.<sup>13</sup> The analysis was carried out with direct methods (SHELX-97<sup>14</sup> or SIR97<sup>15</sup>) using Yadokari-XG.<sup>16</sup> The program ORTEP3<sup>17</sup> was used to generate the X-ray structural diagram. Elemental analysis was performed at the Microanalytical Center of Kyoto University.

**Materials.** Tetrahydrofuran (THF) and triethylamine (Et<sub>3</sub>N) were purified using a two-column solid-state purification system (Glasscontour System, Joerg Meyer, Irvine, CA). 10-Hydroxybenzo[*h*]quinoline,<sup>18</sup> 1,4-diethynyl-2,5-dihexadecyloxybenzene,<sup>19</sup> and 1,4-diethynyl-2-perfluorooctyl-5-trifluoromethylbenzene<sup>20</sup> were prepared according to the literature.

**Synthesis of 1.** Triphenylborane (0.726 g, 3.00 mmol) and 10-hydroxybenzo[*h*]quinoline (0.59 g, 3.00 mmol) were dissolved in toluene (18 mL). After the reaction mixture was refluxed for 12 h, the mixture was allowed to stand for 1 day at –20 °C to precipitate a product. The precipitate was collected by filtration to give a yellow solid in 76% yield (0.82 g, 2.28 mmol). <sup>1</sup>H NMR

\*Corresponding author. E-mail: chujo@chujo.synchem.kyoto-u.ac.jp.

(CDCl<sub>3</sub>,  $\delta$ , ppm): 8.47 (m, 1H, Ar), 8.42 (m, 1H, Ar), 7.84 (dd,  $J = 8.9, 4.8$  Hz, 1H, Ar), 7.72–7.61 (m, 3H, Ar), 7.41 (d,  $J = 8.1$  Hz, 1H, Ar), 7.33 (m, 5H, Ar), 7.24–7.15 (m, 6H, Ar). <sup>11</sup>B NMR (CDCl<sub>3</sub>,  $\delta$ , ppm): 6.55. <sup>13</sup>C NMR (CDCl<sub>3</sub>,  $\delta$ , ppm): 157.81 (Ar), 143.21 (Ar), 140.58 (Ar), 139.78 (Ar), 134.78 (Ar), 133.11 (Ar), 132.82 (Ar), 130.74 (Ar), 127.32 (Ar), 126.58 (Ar), 126.34 (Ar), 123.25 (Ar), 120.74 (Ar), 117.67 (Ar), 116.98 (Ar), 115.26 (Ar). HRMS (EI) Calcd for C<sub>25</sub>H<sub>18</sub>BNO:  $m/z$  359.1481. Found:  $m/z$  359.1478. Anal. Calcd for C<sub>25</sub>H<sub>18</sub>BNO: C, 83.59; H, 5.05; N, 3.90. Found: C, 83.48; H, 5.19; N, 3.77.

**Synthesis of 2.** 9.4 mL (1.6 M, 15 mmol) of *n*-BuLi was slowly added to the solution of 1,4-diiodobenzene (4.95 g, 15.0 mmol) in 75 mL of THF at  $-78$  °C, and the mixture was stirred at  $-78$  °C for 1 h. BBr<sub>3</sub> (0.48 mL, 5.0 mmol) was added to the reaction mixture at  $-78$  °C and then allowed to warm to room temperature and refluxed for 12 h. 10-Hydroxybenzo[*h*]quinoline (0.98 g, 5.00 mmol) dissolved in 15 mL of THF in another flask was added to the reaction mixture and then refluxed for 6 h. The reaction mixture was concentrated under vacuum. The remaining oil was diluted by a small amount of CHCl<sub>3</sub>, and the solution was reprecipitated with 100 mL of methanol to give a yellow solid. This solid was purified by dissolving in a small amount of CH<sub>2</sub>Cl<sub>2</sub> and reprecipitating with 100 mL of hexane to obtain **2** in 53% yield (1.63 g, 2.67 mmol) as a yellow solid. <sup>1</sup>H NMR (CDCl<sub>3</sub>,  $\delta$ , ppm): 8.47 (d,  $J = 7.8$  Hz, 1H, Ar), 8.38 (d,  $J = 4.4$  Hz, 1H, Ar), 7.88 (d,  $J = 9.0$  Hz, 1H, Ar), 7.74–7.65 (m, 3H, Ar), 7.52 (d,  $J = 8.1$  Hz, 4H, Ar), 7.37 (dd,  $J = 7.8, 4.4$  Hz, 2H, Ar), 7.00 (d,  $J = 8.0$  Hz, 4H, Ar). <sup>11</sup>B NMR (CDCl<sub>3</sub>,  $\delta$ , ppm): 6.06. <sup>13</sup>C NMR (CDCl<sub>3</sub>,  $\delta$ , ppm): 157.25 (Ar), 142.80 (Ar), 140.40 (Ar), 140.18 (Ar), 136.44 (Ar), 135.06 (Ar), 134.75 (Ar), 133.00 (Ar), 130.93 (Ar), 126.49 (Ar), 123.30 (Ar), 120.93 (Ar), 118.10 (Ar), 116.94 (Ar), 115.05 (Ar), 93.26 (Ar-I). HRMS (EI) Calcd for C<sub>25</sub>H<sub>16</sub>BI<sub>2</sub>NO:  $m/z$  610.9414. Found:  $m/z$  610.9415. Anal. Calcd for C<sub>25</sub>H<sub>16</sub>BI<sub>2</sub>NO: C, 49.14; H, 2.64; N, 2.29. Found: C, 48.99; H, 2.81; N, 2.29.

**Synthesis of 4O.** Monomer **2** (0.12 g, 0.20 mmol), 1,4-diethyl-2,5-dioctyloxybenzene (0.12 g, 0.20 mmol), CuI (1.9 mg, 0.01 mmol), and Pd(PPh<sub>3</sub>)<sub>4</sub> (12.0 mg, 0.01 mmol) were dissolved in 2.0 mL of THF and 1.0 mL of Et<sub>3</sub>N. After the mixture was stirred at 40 °C for 48 h, a small amount of CHCl<sub>3</sub> was added, and the mixture was poured into a large excess of methanol to precipitate the polymer. The polymer was purified by repeated precipitations from a small amount of CHCl<sub>3</sub> into a large excess of methanol and hexane to give a yellow solid in 72% yield (0.14 g, 0.14 mmol).  $M_n = 10\,800$  g/mol. <sup>1</sup>H NMR (CDCl<sub>3</sub>,  $\delta$ , ppm): 8.46 (1H, Ar), 8.41 (1H, Ar), 7.87 (1H, Ar), 7.72–7.67 (4H, Ar), 7.42–7.36 (6H, Ar), 7.28–7.25 (4H, Ar), 6.93 (2H, Ar), 3.96 (4H, –OCHH<sub>2</sub>–), 1.78 (4H, –CH<sub>2</sub>–), 1.58 (4H, –CH<sub>2</sub>–), 1.47 (4H, –CH<sub>2</sub>–), 1.21 (44H, –CH<sub>2</sub>–), 0.86 (6H, –CH<sub>3</sub>). <sup>13</sup>C NMR (CDCl<sub>3</sub>,  $\delta$ , ppm): 157.52 (Ar), 153.53 (Ar), 143.02 (Ar), 140.53 (Ar), 134.77 (Ar), 132.96 (Ar), 130.90 (Ar), 130.59 (Ar), 126.46 (Ar), 123.27 (Ar), 121.59 (Ar), 120.88 (Ar), 117.97 (Ar), 117.08 (Ar), 115.19 (Ar), 114.09 (Ar), 95.57 (–C≡C–), 85.35 (–C≡C–), 69.62 (–OCH<sub>2</sub>–), 31.93, 29.67, 29.60, 29.38, 29.34, 25.98, 22.70, 14.15. <sup>11</sup>B NMR (CDCl<sub>3</sub>,  $\delta$ , ppm): 4.10. IR (KBr):  $\nu = 3061$  (Ar), 3017 (Ar), 2924, 2853, 2205 (C≡C), 1923 (Ar), 1630 (Ar), 1597 (Ar), 1510, 1468, 1437, 1379, 1342, 1294, 1215, 1148, 1076, 1049, 970, 908, 889, 835, 721 cm<sup>-1</sup>. Anal. Calcd for C<sub>67</sub>H<sub>84</sub>BNO<sub>3</sub>: C, 83.63; H, 8.80; N, 1.46. Found: C, 81.01; H, 8.44; N, 1.46.

**Synthesis of 4F.** Similarly to the preparation of **4O**, **4F** was prepared from monomer **2** (97.8 mg, 0.16 mmol) and 1,4-diethyl-2-perfluorooctyl-5-trifluoromethylbenzene (98.0 mg, 0.16 mmol) in 57% yield as a yellow solid.  $M_n = 6400$  g/mol. <sup>1</sup>H NMR (CDCl<sub>3</sub>,  $\delta$ , ppm): 8.51 (1H, Ar), 8.43 (1H, Ar), 7.89 (2H, Ar), 7.79 (1H, Ar), 7.71 (4H, Ar), 7.40 (5H, Ar), 7.32 (3H, Ar), 7.28 (1H, Ar). <sup>11</sup>B NMR (CDCl<sub>3</sub>,  $\delta$ , ppm): 4.30. IR (KBr):  $\nu = 3065$  (Ar), 3021 (Ar), 2216 (C≡C), 1923 (Ar), 1802 (Ar), 1630 (Ar), 1597 (Ar), 1512, 1441, 1344, 1298, 1244, 1213, 1144, 1078, 1047, 1020, 970, 910, 889, 835, 721 cm<sup>-1</sup>. Anal. Calcd for

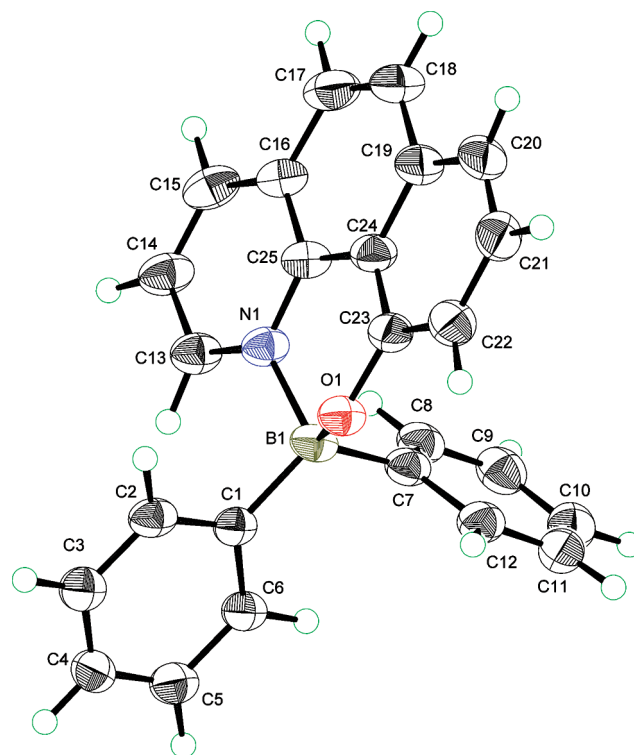
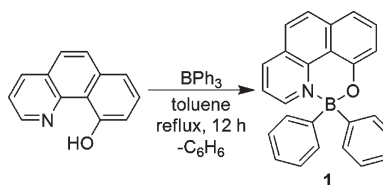


**Figure 1.** X-ray crystal structure of **1** with thermal ellipsoids drawn to the 50% probability level.

#### Scheme 1. Synthesis of Model Compound



C<sub>44</sub>H<sub>18</sub>BF<sub>20</sub>NO: C, 54.63; H, 1.88; N, 1.45. Found: C, 53.98; H, 2.25; N, 1.39.

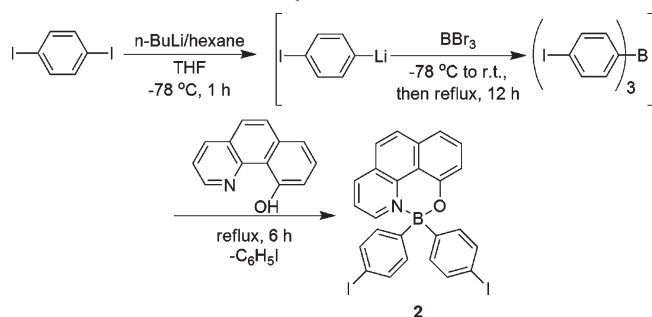
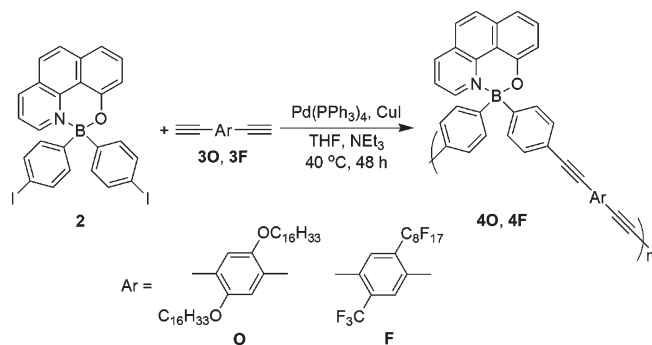
#### Results and Discussion

**Synthesis of Model Compound 1.** The reaction between 10-hydroxybenzo[*h*]quinoline<sup>18</sup> and triphenylborane in toluene under reflux conditions afforded organoboron benzo[*h*]quinolate (**1**) as a yellow precipitate in the reaction mixture at  $-20$  °C (Scheme 1). This compound was stable under air and showed high solubility in dichloromethane and chloroform. The tetracoordination state of the boron atoms in **1** was confirmed by the <sup>11</sup>B NMR spectroscopy in CDCl<sub>3</sub> ( $\delta_B = 6.55$  ppm), and the basic structure was also characterized by <sup>1</sup>H NMR, <sup>13</sup>C NMR, and EI mass spectroscopies and by elemental analysis.

The crystallographically determined molecular structure of **1** is shown in Figure 1. The chelate ring in **1** is six-membered and puckered, differing from that in 8-hydroxyquinolate ligand, with planar five-membered ring. The sp<sup>3</sup> orbital-hybridized boron centers of **1** appear as a slightly distorted tetrahedral geometry with the dihedral angle O(1)–B(1)–N(1) of 105.1° (Table 1), which is closer to an ideal orientation of four sp<sup>3</sup> orbitals than that of B(C<sub>2</sub>H<sub>5</sub>)<sub>2</sub>q (97.0°,  $q = 8$ -hydroxyquinolate)<sup>4</sup> and B(4-iodophenyl)<sub>2</sub>q (99.9°).<sup>10</sup> On the other hand, the angle C(23)–O(1)–B(1) of 117.8° suggested large distortion around oxygen atom of **1**

**Table 1.** Selected Bond Lengths (Å) and Angles (deg) for **1**

B(1)–N(1)	1.635(4)	O(1)–B(1)–N(1)	105.1(2)
B(1)–O(1)	1.500(3)	C(23)–O(1)–B(1)	117.8(2)
O(1)–C(23)	1.358(3)	O(1)–C(23)–C(24)	120.6(3)
C(23)–C(24)	1.415(5)	C(23)–C(24)–C(25)	120.7(3)
C(24)–C(25)	1.441(4)	N(1)–C(25)–C(24)	118.7(2)
N(1)–C(25)	1.369(3)	C(25)–N(1)–B(1)	118.4(2)
B(1)–C(1)	1.602(4)		
B(1)–C(7)	1.613(5)		

**Scheme 2.** Synthesis of Monomer**Scheme 3.** Synthesis of Polymers

as compared with that of  $B(C_2H_5)_2q$  ( $111.8^\circ$ ).<sup>4</sup> The average of  $B(1)–N(1)$  bond length of **1** (1.635 Å) was almost identical to that of  $B(C_2H_5)_2q$  (1.636 Å)<sup>4</sup> and  $B(4\text{-iodophenyl})_2q$  (1.629 Å),<sup>10</sup> probably indicating that 10-hydroxybenzo[*h*]-quinolate possesses high chelating ability as well as 8-hydroxyquinolate.

**Synthesis of Polymers.** Organoboron benzo[*h*]quinolate-based monomer **2** was prepared from 10-hydroxybenzo[*h*]quinoline according to Scheme 2. Compound **2** was obtained as a yellow solid analogous to the model compound when the compound was purified by reprecipitation from methanol and hexane. The monomer was stable under air and soluble in dichloromethane and chloroform. The tetracoordination state of the boron atoms in **2** was confirmed by the <sup>11</sup>B NMR spectroscopy in  $CDCl_3$  ( $\delta_B = 6.06$  ppm), which is similar to the model compound. Moreover, the structure of **2** was also fully characterized by <sup>1</sup>H NMR, <sup>13</sup>C NMR, and EI mass spectroscopies and by elemental analysis.

Scheme 3 and Table 2 summarize the conditions and results for the polymerization of monomer **2** with 1,4-diethynylbenzene derivatives **3O** or **3F** in the presence of a catalytic amount of  $Pd(PPh_3)_4$  and  $CuI$  in the mixed solvent of tetrahydrofuran (THF) and triethylamine. The obtained polymers **4O** and **4F** were collected as yellow solids, and their yields were 72% and 57%, respectively. The <sup>11</sup>B NMR spectra of the obtained polymers were observed at  $\delta_B = 4.10$  ppm (for **4O**) and 4.30 ppm (for **4F**) assignable to the tetracoordination state of the boron atoms in each polymer,

**Table 2.** Polymerization of Organoboron Quinolate-Based Monomers and 1,4-Diethynylbenzene Derivatives<sup>a</sup>

polymer	yield <sup>b</sup> (%)	$M_n^c$ (g/mol)	$M_w^c$ (g/mol)	$M_w/M_n^c$	$DP_n^d$	$T_5^e$ (°C)
<b>4O</b>	72	10 800	25 500	2.4	11.2	298
<b>4F</b>	57	6 400	16 200	2.5	6.6	368

<sup>a</sup> Conditions: Sonogashira–Hagihara couplings of organoboron quinolate-based monomer (1 equiv) and 1,4-diethynylbenzene derivatives (1 equiv) were carried out in the presence of  $Pd(PPh_3)_4$  and  $CuI$  in the mixed solvent (THF/ $NEt_3 = 2/1$ ) at 40 °C for 48 h. <sup>b</sup> Isolated yields after precipitation. <sup>c</sup> Estimated by size-exclusion chromatography (SEC) based on polystyrene standard in tetrahydrofuran (THF). <sup>d</sup> Average number of repeating units calculated from  $M_n$  and molecular weights of repeating units. <sup>e</sup> Thermogravimetric analysis: heating rate 10 K/min under air; values given for weight loss of 5%.

**Table 3.** UV–vis Absorption and Photoluminescence Data

compound	$\lambda_{abs,max}/nm^a$	$\epsilon/M^{-1} cm^{-1} b$	$Ex/nm^c$	$\lambda_{em,max}/nm^d$	$\Phi_F^e$
<b>1</b>	302, 420	3 600	420	513	0.10
<b>4O</b>	314, 373	39 000	373	513	0.16
<b>4F</b>	359, 375	47 700	375	509	0.18

<sup>a</sup> Absorption maxima:  $CHCl_3$  ( $1.0 \times 10^{-5}$  M). <sup>b</sup> Molar extinction coefficients at the longest absorption maxima. <sup>c</sup> Excited wavelength. <sup>d</sup> Fluorescence maxima:  $CHCl_3$  ( $1.0 \times 10^{-5}$  M). <sup>e</sup> Absolute quantum yield.

indicating that the polymerization proceeded without any damage to the structure in the organoboron quinolate moiety. The IR spectra of the polymers showed the absorption peaks at  $2205\text{ cm}^{-1}$  (for **4O**) and  $2216\text{ cm}^{-1}$  (for **4F**), which are attributable to stretching of the  $–C\equiv C–$  bond in the polymer backbone. Moreover, strong broad peaks assignable to the C–F stretching band were observed at around  $1200\text{ cm}^{-1}$  in the spectra of **4F**. The number-average molecular weights ( $M_n$ ) and the molecular weight distributions ( $M_w/M_n$ ) of **4O** and **4F**, measured by size-exclusion chromatography (SEC) in THF, were 10 800 g/mol, 2.4 and 6400 g/mol, 2.5, respectively (Table 2). The degrees of polymerization ( $DP_n$ ) of **4O** and **4F**, estimated by  $M_n$  from SEC, were 11.2 and 6.6, respectively. Thermal stabilities of the polymers were examined by thermogravimetric analysis (TGA) under air. The start of the thermal degradation under air for the polymers **4O** and **4F** lies at 298 and 368 °C, where 5% weight loss was recorded. These data suggest that the obtained polymers present similar thermal stability to general poly(*p*-phenyleneethynylene)s<sup>21</sup> and  $\pi$ -conjugated polymers containing organoboron quinolates in the main chain.<sup>11</sup>

**Optical Properties.** The optical properties of the obtained polymers were investigated by UV–vis absorption and photoluminescence in  $CHCl_3$  solution ( $1.0 \times 10^{-5}$  M) as compared to those of model compounds. The results from the absorption and emission spectra are summarized in Table 3. The model compound **1** showed the weak absorption peaks at 302 and 420 nm arising from the benzo[*h*]quinolate ligand (Figure 2). These peaks stand on the bathochromic side in comparison with those of  $BPh_2q$  (264 and 395 nm). This means that the extension of  $\pi$ -conjugation from quinolate to benzo[*h*]quinolate reduces the width between molecular orbitals and causes the bathochromic shift of the absorption peaks. The polymers **4O** and **4F** exhibited strong absorption bands in the region from 300 to 400 nm like other  $\pi$ -conjugated polymers containing organoboron quinolates in the main chain. Therefore, these bands can be assignable to the  $\pi$ -conjugated linkers connecting the benzo[*h*]quinolate units with each other, and the electronic structure of the  $\pi$ -conjugated linker is also independent from that of the benzo[*h*]quinolate.

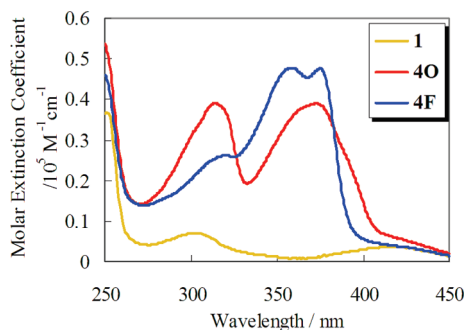


**Figure 2.** UV-vis spectra of polymers and model compound in  $\text{CHCl}_3$  ( $1.0 \times 10^{-5}$  M).

Emission data were obtained after exciting at the longest wavelength of the absorption peaks; i.e., absorption maxima of the polymers and the model compound are corresponding to phenyleneethynylene and benzo[*h*]quinoline, respectively (Figure S1). The spectra of the polymers **4O** and **4F** coincided with its model compound **1**, implying that the polymers emit light from the benzo[*h*]quinolate moiety, and the polymer side chains are nonresponsive to the wavelength of the emission. Although the emission bands of the organoboron benzo[*h*]quinolates were bathochromically shifted as compared with  $\text{BPh}_2\text{q}$ , the Stokes shifts of the former are smaller than that of the latter. In addition, full widths at half-maximum (FWHMs) of the organoboron benzo[*h*]quinolates were narrower than that of  $\text{BPh}_2\text{q}$ . From these results, it can be said that the benzo[*h*]quinolate ligand disturbs the nuclear reorientation and oscillation in the transition state. The photoluminescence property of the model compound **1** in different solvents (THF, DMSO, DMF, and acetonitrile) was also examined. Shifts of the absorption spectra and fluorescence spectra depend on the nature of the solvent, and the solvent polarity greatly affected the Stokes shift. The change in the Stokes shift ( $\Delta\nu$ ) was roughly proportional to the orientational polarizability ( $\Delta f$ ) of the solvent, obeying the dipole interaction theory of Lippert and Mataga (Figure S2).<sup>22</sup> On the basis of this analysis, it can be concluded that the excitation of the organoboron benzo[*h*]quinolate **1** causes ILCT like organoboron quinolate, leading to the charge-separated state. Fluorescence excitation spectra of the polymers in  $\text{CHCl}_3$  ( $c = 1.0 \times 10^{-5}$  M) displayed the similar shapes as the UV-vis absorption spectra; i.e., the strong absorption at  $\pi$ -conjugated linkers in the main chain is crucial in photoluminescence (Figure S3). This suggests that the energy transfer from the  $\pi$ -conjugated linkers to the benzo[*h*]quinolate ligands on the boron centers occurs, followed by photoluminescence from the ligands. Absolute fluorescence quantum yields ( $\Phi_F$ ) of the polymers and the model compound in  $\text{CHCl}_3$  were measured by the integrating sphere method. The quantum yield of **1** ( $\Phi_F = 0.10$ ) is lower than that of  $\text{BPh}_2\text{q}$  ( $\Phi_F = 0.47$ ). The introduction of organoboron benzo[*h*]quinolate into the  $\pi$ -conjugated polymer main chain, however, enhances the quantum yield ( $\Phi_F = 0.16$  or  $0.18$ ). This would mean that the bulky  $\pi$ -conjugated linkers prevent benzo[*h*]quinolate quenching.

**Molecular Orbital Calculations.** To provide more effective understanding for the photophysical behavior of the polymers and the model compounds, we employed the theoretical calculation for compounds **1** and **5** using density-functional theory (DFT) and time-dependent DFT (TD-DFT) method at the B3LYP/6-31G(d)//B3LYP/6-31G(d) level.<sup>23</sup> Figure 3A exhibits HOMO and LUMO of the compound **1**. The geometry optimization of **1** provided the puckered chelate

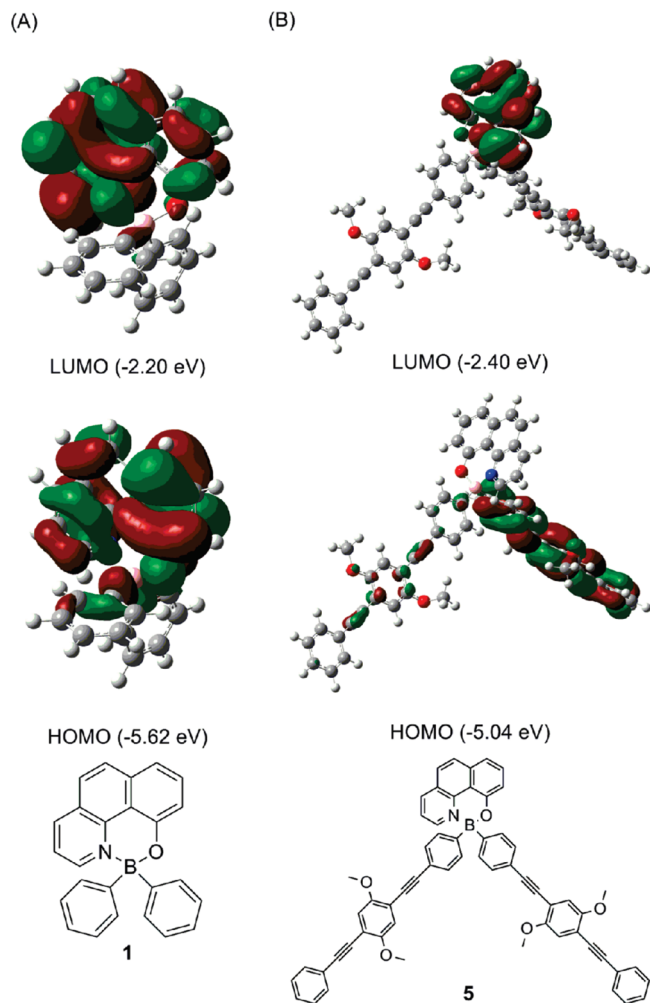


**Figure 3.** Molecular orbital diagrams for the HOMO and LUMO of (A) **1** and (B) **5** (B3LYP/6-31G(d)//B3LYP/6-31G(d)).

ring with boron similar to the X-ray crystal structure. The HOMO of **1** is located predominantly on the phenolate ring, and the LUMO is mainly on the pyridinyl ring. This orbital localization probably causes ILCT as shown in organoboron quinolates. TD-DFT calculation reveals that HOMO-LUMO transition occurs at 431 nm with small oscillator strength ( $f = 0.0618$ ), and this peak position gives good agreement with that of UV-vis spectra (420 nm). In compound **5**, which has  $\pi$ -conjugated linkers, the HOMO is not on the benzo[*h*]quinolate ligand but localized on the one side of the  $\pi$ -conjugated linker and the LUMO is localized on the ligand (Figure 3B). This result supports that  $\pi$ -conjugation is unable to extend through tetracoordinated boron and that the  $\pi$ -conjugated linkers are irresponsible to the electronic structure of the ligand. From the TD-DFT calculation, major oscillator strength of **5** is above 1 at 390 nm ( $f = 1.9901$ ), and this absorption process predominantly consists of the electronic transitions from orbitals on the linker to other orbitals on the linker. This means that the absorption peak of the polymer **4O** at 373 nm is assignable to the  $\pi$ -conjugated linker, and the electronic transition in the linker can more easily take place in comparison with that concerned with the benzo[*h*]quinolate ligand.

## Conclusion

We have successfully prepared the novel low-molecular-mass organoboron benzo[*h*]quinolate complexes (model compound)

and the main-chain-type organoboron benzo[*h*]quinolate polymers. These polymers were obtained by Sonogashira–Hagihara coupling in moderate yields. The emission of the organoboron benzo[*h*]quinolate was responsible for ILCT and shifted to longer wavelength as compared with BPh<sub>2</sub>q. Emission behavior of the polymers was originated from efficient energy transfer from  $\pi$ -conjugated main chain to benzo[*h*]quinolate ligand, and they showed no difference in the emission between donating  $\pi$ -conjugated linker and accepting one. Low-molecular-mass organoboron benzo[*h*]quinolate displayed moderate fluorescence quantum yield ( $\Phi_F = 0.10$ ), and the polymers containing that showed higher quantum yield ( $\Phi_F = 0.16$  or  $0.18$ ).

**Supporting Information Available:** Emission and excitation spectra, Lippert plot, and crystallographic data in CIF format. This material is available free of charge via the Internet at <http://pubs.acs.org>.

## References and Notes

- (1) Haugland, R. P. In *The Handbook—A Guide to Fluorescent Probes and Labeling Technologies*, 10th ed.; Spence, M. T. Z., Ed.; Molecular Probes: Eugene, OR, 2005; Chapter 1, Section 1.4.
- (2) Gorman, A.; Killoran, J.; O'Shea, C.; Kenna, T.; Gallagher, W. M.; O'Shea, D. F. *J. Am. Chem. Soc.* **2004**, *126*, 10619.
- (3) (a) García-Moreno, I.; Costela, A.; Campo, L.; Sastre, R.; Amat-Guerri, F.; Liras, M.; López Arbeloa, I. *J. Phys. Chem. A* **2004**, *108*, 3315. (b) Pavlopoulos, T. G.; Boyer, J. H.; Sathyamoorthi, G. *Appl. Opt.* **1998**, *37*, 7797.
- (4) Wu, Q.; Esteghamatian, M.; Hu, N.-X.; Popovic, Z.; Enright, G.; Tao, Y.; D'Iorio, M.; Wang, S. *Chem. Mater.* **2000**, *12*, 79.
- (5) Tang, C. W.; Vanslyke, S. A. *Appl. Phys. Lett.* **1987**, *51*, 913.
- (6) (a) Cheng, Y. M.; Yeh, Y. S.; Ho, M. L.; Chou, P. T.; Chen, P. S.; Chi, Y. *Inorg. Chem.* **2005**, *44*, 4594. (b) Shi, Y.-W.; Shi, M.-M.; Huang, J.-C.; Chen, H.-Z.; Wang, M.; Liu, X.-D.; Ma, Y.-G.; Xu, H.; Yang, B. *Chem. Commun.* **2006**, 1941.
- (7) (a) Qin, Y.; Pagba, C.; Piotrowiak, P.; Jäkle, F. *J. Am. Chem. Soc.* **2004**, *126*, 7015. (b) Qin, Y.; Kiburu, I.; Shah, S.; Jäkle, F. *Macromolecules* **2006**, *39*, 9041.
- (8) Wang, X.-Y.; Weck, M. *Macromolecules* **2005**, *38*, 7219.
- (9) Nagata, Y.; Chujo, Y. *Macromolecules* **2007**, *40*, 6.
- (10) Nagata, Y.; Otaka, H.; Chujo, Y. *Macromolecules* **2008**, *41*, 737–740.
- (11) Tokoro, Y.; Nagai, A.; Kokado, K.; Chujo, Y. *Macromolecules* **2009**, *42*, 2988.
- (12) Chen, K.-Y.; Hsieh, C.-C.; Cheng, Y.-M.; Lai, C.-H.; Chou, P.-T. *Chem. Commun.* **2006**, 4395.
- (13) Higashi, T. ABCOR. Program for Absorption Correction, Rigaku Corp., Japan, 1995.
- (14) Sheldrick, G. M. SHELX-97. Programs for Crystal Structure Analysis, University of Göttingen, Germany, 1997.
- (15) Altomare, A.; Burla, M. C.; Camalli, M.; Cascarano, G. L.; Giacovazzo, C.; Guagliardi, A.; Moliterni, A. G. G.; Polidori, G.; Spagna, R. *J. Appl. Crystallogr.* **1999**, *32*, 115.
- (16) Wakita, K. Yadokari-XG. Program for Crystal Structure Analysis, 2000.
- (17) Farrugia, L. J. *J. Appl. Crystallogr.* **1997**, *30*, 565.
- (18) Dick, A. R.; Hull, K. L.; Sanford, M. S. *J. Am. Chem. Soc.* **2004**, *126*, 2300.
- (19) Swager, T. M.; Gil, C. J.; Wrighton, M. S. *J. Phys. Chem.* **1995**, *99*, 4886.
- (20) Kokado, K.; Chujo, Y. *Macromolecules* **2009**, *42*, 1418.
- (21) Egbe, D. A. M.; Roll, C. P.; Brickner, E.; Grummt, U.-W.; Stockmann, R.; Klemm, E. *Macromolecules* **2002**, *35*, 3825.
- (22) (a) Lippert, E. Z. *Electrochemistry* **1957**, *61*, 962. (b) Mataga, N.; Kaifu, Y.; Koizumi, M. *Bull. Chem. Soc. Jpn.* **1956**, *29*, 465.
- (23) Frisch, M. J.; Trucks, G. W.; Schlegel, H. B.; Scuseria, G. E.; Robb, M. A.; Cheeseman, J. R.; Montgomery, J. A., Jr.; Vreven, T.; Kudin, K. N.; Burant, J. C.; Millam, J. M.; Iyengar, S. S.; Tomasi, J.; Barone, V.; Mennucci, B.; Cossi, M.; Scalmani, G.; Rega, N.; Petersson, G. A.; Nakatsuji, H.; Hada, M.; Ehara, M.; Toyota, K.; Fukuda, R.; Hasegawa, J.; Ishida, M.; Nakajima, T.; Honda, Y.; Kitao, O.; Nakai, H.; Klene, M.; Li, X.; Knox, J. E.; Hratchian, H. P.; Cross, J. B.; Adamo, C.; Jaramillo, J.; Gomperts, R.; Stratmann, R. E.; Yazyev, O.; Austin, A. J.; Cammi, R.; Pomelli, C.; Ochterski, J. W.; Ayala, P. Y.; Morokuma, K.; Voth, G. A.; Salvador, P.; Dannenberg, J. J.; Zakrzewski, V. G.; Dapprich, S.; Daniels, A. D.; Strain, M. C.; Farkas, O.; Malick, D. K.; Rabuck, A. D.; Raghavachari, K.; Foresman, J. B.; Ortiz, J. V.; Cui, Q.; Baboul, A. G.; Clifford, S.; Cioslowski, J.; Stefanov, B. B.; Liu, G.; Liashenko, A.; Piskorz, P.; Komaromi, I.; Martin, R. L.; Fox, D. J.; Keith, T.; Al-Laham, M. A.; Peng, C. Y.; Nanayakkara, A.; Challacombe, M.; Gill, P. M. W.; Johnson, B.; Chen, W.; Wong, M. W.; Gonzalez, C.; Pople, J. A. *Gaussian 03, revision D.01*; Gaussian, Inc.: Wallingford, CT, 2004.